Fluid Mechanics of DNA Double-Strand Filter Elution

George Rudinger* and Ed Robert Blazek†
*Department of Mechanical and Aerospace Engineering, State University of New York at Buffalo, Buffalo, New York 14260; and
†Department of Radiation Oncology and Medical Physics, Rush University, Chicago, Illinois 60612 USA

ABSTRACT Measurement of infrequent DNA double-strand breaks (DSB) in mammalian cells is essential for the understanding of cell damage by ionizing radiation and many DNA-reactive drugs. One of the most important assays for measuring DSB in cellular DNA is filter elution. This study is an attempt to determine whether standard concepts of fluid mechanics can yield a self-consistent model of this process. Major assumptions of the analysis are reptation through a channel formed by surrounding strands, with only strand ends captured by filter pores. Both viscosity and entanglement with surrounding strands are considered to determine the resistance to this motion. One important result is that the average elution time of a strand depends not only on its length, but also on the size distribution of the surrounding strands. This model is consistent with experimental observations, such as the dependence of elution kinetics upon radiation dose, but independence from the size of the DNA sample up to a critical filter loading, and possible overlap of elution times for strands of different length. It indicates how the dependence of elution time on the flow rate could reveal the relative importance of viscous and entanglement resistance, and also predicts the consequences of using different filters.

INTRODUCTION

DNA damage, in particular the DNA double-strand break (DSB), is the principal lethal or mutagenic lesion produced in cells by ionizing radiation (Painter, 1980) and certain cancer therapeutic drugs such as bleomycin and etoposide (Simon et al., 2000). Mammalian cells devote at least three distinct multi-enzyme systems to the biochemical repair of DSB (Dasika et al., 1999), and cells that are deficient in one or more of these enzymes are usually hypersensitive to killing by such agents (Boulton et al., 2000). Much effort has been directed toward measurement of DSB produced by clinically relevant doses of radiation and drugs. Such measurements should be valuable, in part, for insights into fundamental mechanisms of cancer cell killing by radiation and drugs. In addition, it is possible that residual DSB frequency could be used to predict clonogenic cell survival accurately enough to serve as a surrogate survival endpoint (Kiltie et al., 1997). This would be valuable to predictive testing of cancer therapies because DSB residues can be measured in less than a week, rather than the 3–5 weeks required by direct colony-forming assays (West, 1995).

The first reasonably sensitive assays for DNA damage in mammalian cells were based upon velocity sedimentation through sucrose gradients (Lett et al., 1967). Radiation doses in excess of 200 Gy were generally required for reproducible measurement of DSB by velocity sedimentation. A mathematical theory of velocity sedimentation was developed by Zimm (1974) and Zimm and Schumaker (1976). Their theory of deformable random coils accounts quantitatively for the observed phenomena, explaining the rotor speed-dependence of sedimentation velocity and other subtle features of assay behavior.

In the 1970s Kohn and co-workers (1973, 1976) developed filter elution assays, initially for total strand breaks (single- plus double-strand breaks) at a pH sufficient to denature the strands (pH $>$ 12), then specifically for DSB at near-neutral pH (Bradley and Kohn, 1979). The principle of filter elution is that the rate at which DNA strands are carried through a microporous filter by a fluid flow depends upon the length distribution of those strands. Filter elution is superior to velocity sedimentation with respect to sensitivity, equipment cost, and number of samples that can be analyzed.

Agarose gel electrophoresis, in which DNA molecules are driven through a size-discriminating gel by an electric field, resolves molecules of kilobase-pair (kbp) lengths but is unable to discriminate between Mbp-sized DNA fragments when operated with a constant electric field (McDonell et al., 1977). Schwartz and Cantor (1984) introduced the concept of pulsed-field gel electrophoresis (PFGE), in which the direction of the electric field was periodically reoriented to induce differences in the mobility of Mbp-length DNA molecules such as yeast chromosomes. Some more recent versions of PFGE can detect DSB produced by only 1–2 Gy (Nevaldine et al., 1997). PFGE was the most sensitive DSB assay until Kaur and Blazek (1997) showed that the sensitivity of neutral filter elution could be improved by increasing the pH to 11.1, just below the DNA denaturation value. At this pH, filter elution is as sensitive as PFGE and avoids artifacts of PFGE for measurement of the kinetics of DSB rejoining. Both constant-field and pulsed-field gel electrophoresis have been modeled with considerable success using the concept of reptation, in which the DNA molecules move through tubes established by the gel structure (de Gennes, 1971; Duke et al., 1996; Kantor et al., 1999).

Received for publication 12 February 2001 and in final form 18 September 2001.

Address reprint requests to Dr. George Rudinger, 47 Presidents Walk, Buffalo, NY 14221. Tel.: 716-689-9570; E-mail: rudinger@acsu. buffalo. edu.

0006-3495/02/01/19/10 $2.00

In contrast to velocity sedimentation and gel electrophoresis, there is no generally accepted mathematical model for the filter elution assay. Nicolini et al. (1983) and Balbi et al. (1986) developed models based on the assumption that individual strand fragments form isolated random coils represented by equivalent solid spheres that gradually are swept through the filter pores. Kohn (1991) believed that these models were implausible because at the high DNA concentrations on the filter, ideal random-coil configurations would be approached only very slowly, if at all, and in any case such configurations would be readily distorted by the flow. These theories also predicted a critical dependence of elution rate on the size of the filter pores, which he did not observe. Instead, Kohn (1979, 1991) postulated that the fluid pulls a strand into several pores to form competing loops; the longer loops then pull the shorter ones back through the filter until, finally, one loop overwhelms all the others and pulls the strand through. This process was nicknamed the "tug-of-war" model by Mayer et al. (1991), but their experiments provide only partial support. Kohn (1991) refers to his own modeling attempts based on the tug-of-war model; he gives no details, but a later review of his work (Kohn, 1996) does not refer to these efforts.

Elution of single-stranded DNA requires prior denaturation, or unwinding, of the DNA double helix. The DNA denaturation rate depends on fragment length; in fact, the alkaline unwinding assay for single-strand breaks is based on this principle (Ahnstrom and Erixon, 1973). We do not include the unwinding time in our model; therefore, our model applies only to double-strand elution. All experimental data used in the following were obtained with a pH 11.1 elution fluid, for which the two strands of the DNA double helix do not separate (Kaur and Blazek, 1997). The possibility that double-strand DNA molecules might have short single-stranded ends will be discussed below.

The present analysis attempts to use standard concepts of fluid dynamics to explain experimental observations. Elution is an example of two-phase flow; that is, of a continuum flow of a liquid or a gaseous phase interacting with a dispersed phase consisting of solid particles of various sizes and shapes, liquid droplets, or gas bubbles. Depending on the velocity of the continuum flow, the nature and mass fraction of the dispersed phase and the importance of interaction between elements of the dispersed phase, many different flow patterns can arise, each requiring its own analysis. Two-phase flows are frequently encountered, such as blood flow, sprays, transport of granular materials through pipelines, and exhaust from diesel engines. The extensive literature includes, for example, Clift et al. (1978), Rudinger (1980), Crowe et al. (1997), Fuchs (1989), and Fan and Zhu (1998). One feature common to these flows is that the two phases can have different velocities, and that the resulting viscous interaction—the drag—tends to equalize the velocities. Also, with very few exceptions, the drag cannot be computed directly but must be derived from experimental data obtained either in the flow being studied or in properly simulated flows.

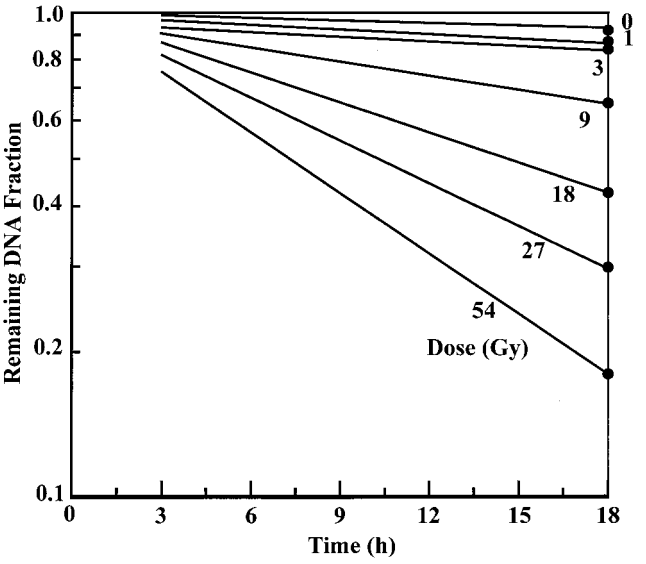

FIGURE 1 Decrease of Q_R with time for several experimental radiation exposures. The lines are based on the "smoothed" experimental values of $Q_R(18)$ marked on the right edge (see Fig. 2).

Elution analysis

Experiments with human DNA (Kaur and Blazek, 1997) yielded the expected result that the fraction Q_R of DNA retained on the filter can be approximated by an exponential decrease with time

$$Q_R = \exp(-K * T_E) \quad (1)$$

where T_E is the elution time, and the constant K depends on the radiation exposure. These results are shown in Fig. 1, where the remaining DNA fraction is plotted as a function of time. To eliminate effects of experimental scatter, the plot is based on "smoothed" 18-h values $Q_R(18)$. These are obtained from a plot like Fig. 2, which shows a curve visually fitted to the experimental data points. Experimental and smoothed values of $Q_R(18)$ are collected in Table 1. Also included are the values of K obtained from the smoothed values of $Q_R(18)$ and from Eq. 1 as

$$K = -\ln[Q_R(18)]/18 \quad (2)$$

The results for 0 Gy indicate that the DNA sample used must have included either unbroken strands short enough to elute during the experiment or previous strand breaks of unknown origin. As indicated by the following model calculations, the length of any fragments that have an average elution time of 18 h or less is at most 1.3 cm. By comparison, the human genome, which has a length of 102 cm, consists of 24 chromosomes between 1.94 and 8.61 cm

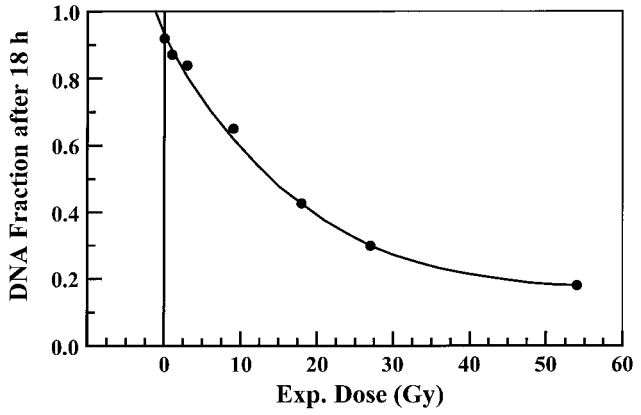

FIGURE 2 Dependence of $Q_R(18)$ on the experimental exposure. The curve is a fit to the marked experimental points and extrapolated to $Q_R(18) = 1.0$.

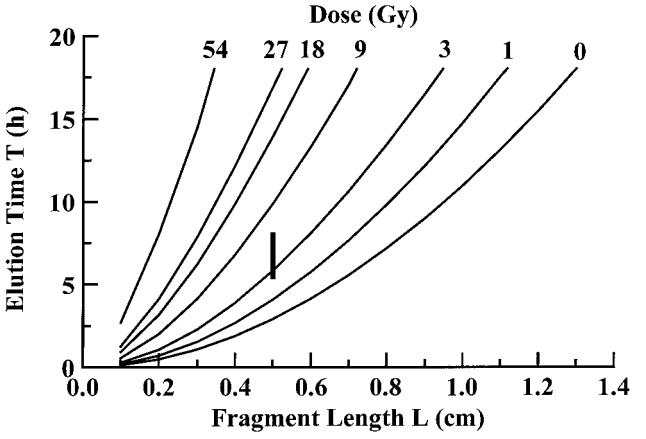

FIGURE 3 Calculated elution times T_E for DNA fragments of length L produced by various radiation exposures. All curves are terminated when the elution time reaches 18 h, the standard duration of an experiment. The heavy vertical line represents an example of elution-time overlap for $L =$ 0.5 cm and 3-Gy exposure, as discussed in the text.

long, and the shortest chromosome, no. 22, represents only 1.9% of the total genomic DNA. Thus few, if any, undamaged strands could have eluted in the manner described by Eq. 1, and there must have been pre-elution breaks either naturally present or as the result of handling, self-irradiation from the radioactive label (Burki et al., 1975), or other causes. This apparent breakage is unlikely to be due to replication intermediates, however, since all such intermediates that incorporate radioactive label will have time to become full-length DNA, and those that do not incorporate label are invisible to the experiment.

These breaks may or may not be randomly distributed, but for the purpose of elution modeling it is assumed that they can be adequately described as if they had been produced by an equivalent radiation exposure. Because of such uncontrollable breaks, samples with different "histories" may yield slightly different results, and it is important for modeling that all experimental data used are based on DNA from the same source. Extrapolation of the data in Table 1 to $Q_R(18) = 1.0$, shown in Fig. 2, indicates that this equivalent pre-elution exposure for the experiments used here is ~1 Gy, and the size distribution of DNA fragments, therefore, is based on a DOSE equal to the experimental dose plus 1 Gy.

According to the foregoing, a relationship is needed between the length of a DNA fragment and its elution time.

TABLE 1 Basic data

Dose	Experimental $Q_R(18)$	Smoothed $Q_R(18)$	K (h^{-1})
0	0.919	0.930	0.00403
1	0.871	0.885	0.00679
3	0.839	0.805	0.0121
9	0.650	0.619	0.0266
18	0.426	0.426	0.0474
27	0.299	0.299	0.0671
54	0.180	0.180	0.0953

This can be obtained with the help of the random distribution of strand breaks developed by Contopoulou et al. (1987). After correcting a misprint in this paper, Cedervall and Källman (1995) derived the equation

$$Q = 1 - \exp(-\mu * L/L_T) * [1 + \mu * L/L_T * (1-L/L_T)] \quad (3)$$

where Q is the fraction of DNA contained in all strand fragments up to length L, L_T is the undamaged length, and μ is the average number of DSB. They also pointed out that a human genome, "with chromosomes covering a limited range, can be represented by a single large chromosome." After the fragments up to length L have eluted, the remaining fraction can be obtained from Eq. 3 as $Q_R = 1 - Q$, and the corresponding elution times then follow from Eq. 1. The calculations are based on a radiation sensitivity reported by Löbrich et al. (1994) as 5.4 DSB Gbp^{-1} Gy^{-1}, so that $\mu(DSB) = 5.4 * LT(Gbp) * DOSE(Gy)$, where DOSE is the experimental dose plus 1 Gy, K is given in Table 1, and according to the foregoing, on $L_T = 102/24 = 4.25$ cm = 0.125 Gbp. Results of these calculations, shown in Fig. 3, indicate that the elution time of a strand fragment depends not only on its length, but also on the radiation exposure. Since higher exposures produce more breaks, one is led to the conclusion that more and shorter fragments get more entangled than the original strands; the result is higher resistance to strand motion and, consequently, longer elution times.

The Nucleopore polycarbonate filter used (Corning Costar Corp., Cambridge, MA) has a pore density of $N =$ 3E7 pores/cm^2 and pores of diameter $p =$ 8E-5 cm. Flow through the filter is distributed over 30 holes of 0.18-cm diameter in a 0.25-cm-thick support plate (Swinnex

SX0002500, Millipore Corp., Bedford, MA), which has a series of fine concentric ridges to prevent the solid plate portion from blocking flow through some filter pores. For the normal flow rate of 2 ml/h, the velocity is $U_0 = 0.504$ cm/h above the filter and $U = 2.52$ cm/h in the holes. Behind the support plate, the available cross-section increases discontinuously to the total filter diameter of 2.2 cm. Flows from the holes emerge as jets, but the velocity becomes uniform after a short distance. The distance to the final exit tube of 0.2-cm diameter is ~1 cm, but this passage has a complicated shape with conical, cylindrical, and curved wall segments, a discontinuous area change, and several small ridges to hold the filter support plate. Therefore, the velocity behind the filter support plate is smaller than the velocity in the holes, but it becomes larger toward the end of the passage. To avoid the problem of the uncertain velocity variations along the strand, an effective average velocity over the entire length of the eluted strand portions is assumed to equal the velocity in the holes, but acting only on the strand to a maximum distance $X_M = 0.5$ cm from the filter. (The consequences of choosing other values of X_M are discussed below.) Because of this assumption, the model leads to a discontinuous change in the rate at which some quantities vary when the eluted strand portion becomes longer than X_M, but because the force is not actually discontinuous, the discontinuities indicated by the calculations would not appear in experimental data. Since a strand on the filter crosses all pores that have their center within a band of width p along the contour of the strand, the number of these pores is $N * p = 2400$ pores per cm for the filter used. Thus, the average distance between neighboring pores along the strand is only $s = 4.2\text{E-}4$ cm.

Consider first a straight isolated strand of length L captured by only one pore, and let X be the portion that has passed through the filter; then, $V = dX/dT$ is the strand velocity. The viscous drag acting on X produces the driving force for the motion. This strand portion may be considered a highly elongated ellipsoid, one of the few cases for which Oberbeck, in 1876, quoted by Clift et al. (1978), derived the shape correction factor for the classical Stokes drag of a sphere in slow motion relative to a fluid. Fuchs (1989) suggested a simplification for extremely long needle-shaped ellipsoids aligned with the flow. In terms of the variables used here, the driving force in dynes is

$$F_D = 2\pi * \eta * (U - V) * X/[\ln(2 * X/D) * 3600] \quad (4)$$

where $\eta = 0.011$ dyne $*$ s/cm^2 is the viscosity of the fluid, $D = 2.5\text{E-}7$ cm is the strand diameter, and the factor 3600 is needed because velocity is measured in cm/h. The diameter that should be assumed for DNA merits discussion. Although the diameter across the phosphodiester backbone is 2.2E-7 cm, the hydrodynamic DNA diameter as determined by sedimentation analysis is 2.6E-7 cm (Gray et al., 1967). We have chosen an intermediate value closer to the hydrodynamic value, but it is worth noting that the diameter appears only as the argument of the logarithm throughout this analysis, so the numerical effect of this uncertainty is negligible.

The resisting force is given by a similar equation, but the affected strand portion is now $L - X$, and the relative velocity is just V, because there is no net flow in the direction of the strand motion. Thus, the resisting force becomes

$$F_R = 2\pi * \eta * V * (L - X)/\{\ln[2 * (L - X)/D] * 3600\} \quad (5)$$

The equation of motion for an isolated strand captured by one pore then is

$$m * d^2X/dT^2 = F_D - F_R \quad (6)$$

where m is the mass of the strand. It is convenient to introduce the function

$$G(Z) = Z/\ln(2 * Z/D) \quad (7)$$

which can be approximated within a factor of ~3 by $G(Z) = Z/6$ over the entire range of interest. With this approximation, the equation of motion for an isolated strand becomes

$$d^2X/dT^2 + \beta * dX/DT - \beta * U/L * X = 0 \quad (8)$$

where $\beta = 1200\pi * \eta * L/\text{m h}^{-1}$. The solution of this equation, for the initial conditions $X = X_0$ and $dX/dT = 0$ at $T = 0$, is given by

$$X = X_0 * \{(\beta + U/L) * \exp(U * T/L) + (U/L) * \exp[-(\beta + U/L) * T]\}/(\beta + 2 * U/L) \quad (9)$$

Since m is proportional to D^2, the value of β is ~13 orders of magnitude larger than U/L, and some terms in Eq. 9 can be neglected. Then, Eq. 9 is simplified to

$$X = X_0 * \exp(U * T/L) \quad (10)$$

The same solution could have been obtained directly by setting $m = 0$ in Eq. 6. Then, only the force balance $F_D = F_R$ remains, and the differential Eq. 8 is reduced from second to first order, so that only one initial condition, $X = X_0$ for $T = 0$, can be satisfied. This result means that the inertia of the strand is so small that the strand always moves with the velocity at which the driving and the resisting forces are equal: the motion is quasi-steady. For $X_0 = s$, even this crude approximation yields elution times of the right order of magnitude. The strand velocity follows from Eq. 10 as

$$V = dX/dT = (X_0 * U/L) * \exp(U * T/L) \quad (11)$$

It does not satisfy the initial condition $V = 0$, but the approximation is very good, because X_0/L is extremely

small. This example indicates that using a force balance is a promising approach for elution modeling.

The foregoing example implies that all parts of a strand move with the same velocity. It is well established that a strand pulled by one end from a sample of DNA moves in snake-like fashion along its contour in a channel formed by surrounding strands. This motion, known as reptation, was analyzed by de Gennes (1971) and experimentally observed for isolated DNA by Perkins et al. (1994) and for DNA undergoing gel electrophoresis (Duke et al., 1996; Kantor et al., 1999). We assume that both strand ends are captured by the nearest pores they encounter to form the initial overhangs X_0 and Y_0, after which all subsequent strand motion occurs via reptation. It should be noted that these assumptions are incompatible with the "tug-of-war" model, in which portions of the strand between the ends would also be captured by pores, causing different portions of the strand to move at different velocities.

A strand end that happens to be within a filter pore would rapidly form the initial overhang. If the end were outside a pore, its distance from the nearest pore would not exceed s, the distance between neighboring pores, and only a small motion of the end without motion of the entire strand would be needed to form the overhang. The time required to form the overhang is of the order of s/U_0, and the velocity increases as the flow approaches a pore. We will not consider this time, although there are some conditions that could alter it significantly.

If a double-strand break is two-hit (formed by nearly overlapping single-strand breaks on opposite strands) or a staggered one-hit DSB, the ends of a molecule will have short single-stranded segments. Single-stranded ends could affect the elution kinetics of long double-stranded molecules if 1) the ends bind chemically to the filter material, or 2) if by their flexibility, they accelerate strand capture. The first possibility is excluded by the fact that single-stranded elution kinetics are insensitive to filter composition (Kohn et al., 1976). The second possibility could be tested by comparing the elution kinetics of DNAs treated with blunt-end-producing and staggered-end-producing restriction endonucleases. Once strands are captured, however, the single-stranded ends should have little or no further effect on elution kinetics.

Motion of a strand under the influence of opposing driving and resisting forces implies that the initial overhangs X_0 and Y_0 must be different. Even if X_0 and Y_0 were equal, the slightest disturbance would make one overhang larger than the other, and the strand would no longer be trapped on the filter. With the convention $X_0 > Y_0$, the drag on the X overhang is the driving force, given by Eq. 4, while the drag on the Y overhang, which is being pulled back toward the filter, contributes to the resistance. Drag from the Y overhang is similar to Eq. 4 with V replaced by $-V$ and X replaced by Y. The rest of the strand, $L_R = L - X - Y$, will be referred to as the resistance length. It produces additional resistance that results from friction between touching strands moving relative to each other in addition to a viscous drag from the strand moving through the fluid. In analogy to Eq. 4, this resistance is defined as

$$F_R = (R_E + R_V) * V * L_R/3600 \qquad (12)$$

where R_E is the resistance from the friction between entangled strands per unit velocity and per unit resistance length, and R_V is the corresponding contribution from the viscous interaction between the strand and the fluid.

Experimentally, the rate of elution at pH 11.1 is nearly independent of the number of cells loaded per filter for fewer than approximately one million cells, after which the rate of elution becomes slower (Kaur and Blazek, 1997). Studies of DNA electrophoresis through a regular array of pins formed from silicon reveals that DNA moves by reptation through this array. When a force transverse to the instantaneous orientation of the strand is applied by changing the direction of the electric field, reorientation occurs at a rate that is extremely sensitive to the lattice spacing, with a sudden transition occurring when the applied force exceeds a value proportional to (lattice spacing)$^{-3}$ (Duke et al., 1996). Because the lattice in filter elution comprises the DNA itself, an increase of DNA loading above a critical value would be expected to sharply increase the time necessary for a strand end to reorient toward a nearby pore in the filter. Thus, the reptation model is at least qualitatively consistent with loading-independence of elution rate up to a critical threshold, followed by a sudden slowing of elution.

There is little prospect that a theoretical prediction for the variables R_E and R_V will become available, but at least their dependence on flow rate and viscosity of the elution fluid can be assessed. Entanglement resistance results from the friction between strands pressed against each other by the drag of the flow across the strands into the filter; it is, therefore, proportional to the velocity and viscosity of the fluid. In contrast, the viscous part of the resistance is proportional only to the viscosity. Therefore, let $R_E = f_E * M * \eta$ and $R_V = f_V * \eta$, where f_E and f_V are the unknown terms of the resistance components for flow at 2 ml/h, and M is the actual flow rate divided by 2 ml/h. All numerical results presented in the following are based on $M = 1$; hence the flow rate used in the present experiments was 2 ml/h. Since a strand is assumed to move as one unit, any increase of X results in an equal decrease of Y, so that

$$X + Y = X_0 + Y_0 = X_1 = \text{const.} \qquad (13)$$

Decrease of Y can continue only until $Y = 0$. Then, the drag on X continues to provide the driving force, while the strand motion prevents reestablishment of a new Y overhang at another pore. Accordingly, elution takes place in two stages: stage 1 with strand motion in two pores and stage 2 in only one pore. For stage 1, the driving force is given by Eq. 4, and the two parts of the resistance by Eq. 4, modified for the

Y overhang as indicated in the foregoing, and by Eq. 12 for the contribution from the resistance length. The force balance, including the factor M, thus becomes

$$2\pi * \eta * (U * M - V) * G(X) = (R_E + R_V)V * L_R + 2\pi * \eta * (U * M + V) * G(Y) \quad (14)$$

where Eq. 7 also has been used. Solving for V yields

$$V = U * M * \frac{G(X) - G(Y)}{G(X) + G(Y) + R * L_R} \quad (15)$$

where $L_R = L - X_1 = \text{const.}$, $Y = X_1 - X$ from Eq. 13, and R is a dimensionless resistance parameter defined by

$$R = (R_E + R_V)/(2\pi * \eta) = (f_E * M + f_V)/(2\pi) \quad (16)$$

Note that, since all forces acting on a strand are proportional to the viscosity, this variable does not appear in these equations, and the strand motion becomes independent of viscosity! Our attempts to increase the viscosity of the elution solution by adding sucrose or glycerol and adjusting the pH were inconclusive, probably because of some chemical effect of these additives.

It is now possible to compute the strand velocity for any value of X. However, the purpose of the analysis is not to find V as a function of X, but X as a function of the time at which the strand reaches the position X. This time can be obtained by performing a simple numerical integration of $dT = dX/V$ in small steps H of X starting with $X = X_0$ for $T = 0$. For each step, V is taken as the average of the beginning and end values for the step. Then, X is increased and Y decreased by H until the end of stage 1, where $Y = 0$ and $X = X_1$; the corresponding time is denoted T_1. Omitting all Y-terms in Eq. 15 yields the force balance for stage 2 as

$$V = U * M/[1 + R * L_R/G(X)] \quad (17)$$

where now $L_R = L - X$. The velocity again is determined for any value of X, and the corresponding time by integration continuing from the end values X_1 and T_1 from stage 1. In the evaluation of V, $G(X)$ becomes $G(X_M)$ whenever X exceeds X_M according to the assumption made that the driving force acts on X only up to $X = X_M$. These steps must be repeated to the end of stage 2, where $X = L$, $V = U$, and $T = T_M$. The notation T_M is used for the model elution time to distinguish it from the experimental time T_E. A small initial step size $H =$ 1E-6 cm is used, but every subsequent step size is increased by 10% until the step reaches 1% of L and is kept at that value for the rest of the calculations. If a step size leads to X exceeding the known end value for the stage (X_1 for stage 1 and L for stage 2), it is adjusted to produce the correct end value.

The foregoing computational procedure involves the three as yet unspecified parameters R, X_0, and Y_0. For the model calculations, R is obtained by computing T_M based on a guess for R that is varied until T_M and T_E agree to within 0.001 h. The need to use experimental data for the evaluation of drag in two-phase flow was mentioned earlier. The choice of X_0 and Y_0 is based on the assumption that the initial overhangs X_0 and Y_0 have a random value between zero and a maximum $X_{0M} = s$, the distance between neighboring pores that are crossed by a strand, with the restriction $X_0 > Y_0$. The calculations then are based on the average of all possible combinations of X_0 and Y_0 between 0 and X_{0M}. To determine this average, the range from 0 to 1 is divided into N equal segments and their end points marked 0, 1, . . . , N. Any number, I for X_0 and J for Y_0 with $I > J$, when divided by N, can identify a possible fraction of X_{0M} as an initial overhang. Consequently, the calculations are based on $X_0 = X_{0M} * A$ and $Y_0 = X_{0M} * B$, where A and B are the averages of all values of I/N and J/N as N goes to infinity. All possible pairs I, J defined in this manner are collected in the array in Table 2. There are N columns each with a constant I, and N lines each with a constant J. To obtain the average I, the sum of all I's must be divided by the sum of all I, J pairs in the array. The latter is given by

TABLE 2 Array of all pairs *I*, *J*

1, 0	2, 0	3, 0	N-1, 0	N, 0
	2, 1	3, 1	N-1, 1	N, 1
		3, 2	N-1, 2	N, 2
		.	.	
		.	.	
		.	.	
			$N - 1, N - 2$	$N, N - 2$
				$N, N - 1$

$$S(P) = 1 + 2 + 3 + \cdots + N = N * (N + 1)/2 \quad (18)$$

and, since the number of pairs in each column equals the value of I in that column, the sum of all I's is

$$S(I) = 1^2 + 2^2 + 3^2 + \cdots + N^2 = N * (N + 1) * (2N + 1)/6 \quad (19)$$

(e.g., Dwight, 1953). Thus, one obtains $A = S(I)/[S(P) * N] = (2N + 1)/(3N)$, which for large N becomes ⅔. In the same manner, the sum of all J's is

$$S(J) = N * 0 + (N - 1) * 1 + (N - 2) * 2 + \cdots + 2 * (N - 2) + 1 * (N - 1) \quad (20)$$

which can be written as

$$S(J) = S[(N - K) * K] = N * S(K) - S(K^2) \quad (21)$$

where K varies from 0 to $N - 1$. The summations as in Eqs. 18 and 19 yield

$$S(J) = N * (N^2 - 1)/6 \quad (22)$$

After division by $S(P)$ and N as before, the average $B = (N - 1)/(3N)$ is obtained, which for large values of N

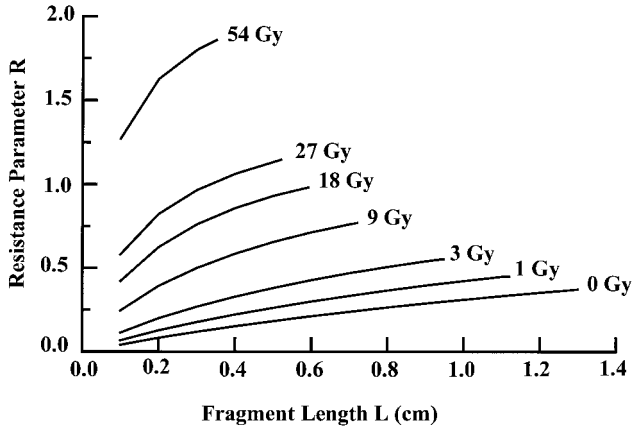

FIGURE 4 Average resistance parameter R for DNA fragments produced by various radiation exposures. The ends of the curves indicate that the elution time has reached 18 h. The effect of eliminating the restriction on $X_M = 0.5$ cm is too small to show in the figure.

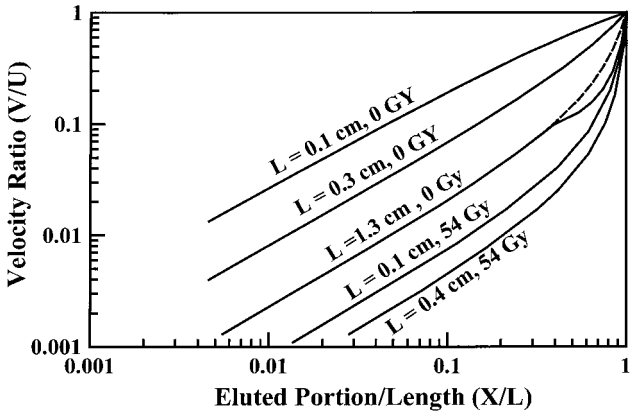

FIGURE 5 Relationship between the calculated fragment-to-fluid velocity ratio V/U and the fraction of eluted fragments X/L for the indicated fragment lengths and dose. The solid lines are based on $X_M = 0.5$ cm, and the dashed line represents one example without this restriction.

converges to $B = ⅓$. Therefore, all calculations are based on the initial values $X_0 = (⅔) * X_{0M}$ and $Y_0 = (⅓) * X_{0M}$. Incidentally, this result shows that $X_1 = X_{0M}$ according to Eq. 13.

A consequence of the range for the initial overhangs is that the elution time of one strand can be greater than that of a longer strand. An example of this "overlap" is shown in Fig. 3, as a heavy line, for $L = 0.5$ cm and a 3-Gy exposure. The average elution time for this case is 5.83 h. The minimum time, for $X_0 = X_{0M}$ and $Y_0 = 0$, is 5.47 h. The maximum time is infinite when $X_0 = Y_0$, but because equal overhangs are unstable, the upper limit, shown for $X_0 =$ 1E-6 cm and $Y_0 = 0.9999$E-6, is ~8 h.

The results in Fig. 4, based on the data in Table 1 and $M = 1$, show the dependence of R on fragment length L for several experimental radiation exposures and for elution times up to 18 h. The increase of R along each curve indicates a tightening of the entanglement resulting from the interacting DNA strands. If the limit $X_M = 0.5$ cm is removed by making X_M equal to or greater than L, the effect on R is <2%, too small to be shown in the figure.

Strand velocity is given by Eqs. 15 and 17, and the velocity ratio V/U during elution is shown in Fig. 5. The velocity increases about linearly with X as long as X/L is <~0.2, and then more and more rapidly until $V/U = 1$ at $X/L = 1$. For a given fragment length the velocity is lower, and thus the elution time longer, if the fragment is from the sample that received more radiation; for a given radiation exposure the velocity is higher for the shorter strand. These results are in agreement with the results in Figs. 3 and 4. For the longest fragments, which are the ones most affected by the assumption for X_M, results are shown for $X_M = 0.5$ cm and $X_M = L$ (*dashed line*). The two curves are identical as long as $X < X_M$ and separate near $X/L = 0.4$, but the effect is small. A consequence of using the force balance instead of the complete equation of motion is that the initial condition of zero velocity cannot be exactly satisfied, but the computed maximum initial velocity never exceeds 0.004 cm/h for all cases considered.

The earlier discussion of the resistance parameter, R, suggests an experiment to determine its components R_E and R_V. If the values of R were determined for two flow rates, then Eq. 16 would provide two equations for the unknown values of f_E and f_V. If the entanglement resistance were considerably greater than the viscous resistance, the elution time would be only weakly dependent of the flow rate. Such results have actually been reported by Kohn (1979, 1996) for single-strand elution, and are predicted by the present model also for double-strand elution. In the absence of suitable experimental data it can be stated only that the importance of R_E relative to R_V increases with the flow rate.

Another incidental result of the model is strand tension. The driving and resisting forces are distributed over the entire affected portion of the strand, with the tension being zero at the ends and increasing along the strand to a maximum at the filter pore. This maximum thus is equal to the driving force given by Eq. 4. In Fig. 6 the tension in picoNewtons (pN) is shown as a function of time for the case of zero exposure (longest strands) and fragment lengths of 0.5, 1.0, and 1.3 cm. Tension increases from a low value to a maximum near the end of elution and then rapidly drops back to zero. The distortions near the peak of the curves for the two longer fragments clearly are a consequence of the assumption $X_M = 0.5$ cm. There is no distortion if this restriction is eliminated (*dashed lines*), but the numerical results then suffer from the uncertainty of the flow velocity in the filter holder. Results for higher exposures are similar, but the distortions become less pronounced and disappear for 54 Gy, for which the fragments are too small to be affected. This modeling complication could be eliminated

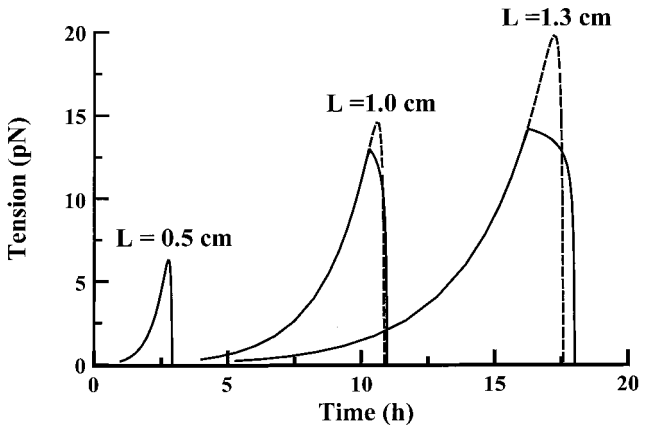

FIGURE 6 Maximum strand tension during elution for three fragment lengths L and 0-Gy exposure. The solid lines are based on $X_M = 0.5$ cm, while the dashed lines are examples for $X_M = L$.

if, in future experiments, the present filter support plate were replaced by a block as thick as the longest strand fragments, so that the flow velocity would be well defined. A review of the elastic properties of DNA by Austin et al. (1997) states that 50 pN would stretch DNA beyond its natural length by ~10%. Near 70 pN, DNA abruptly yields and expands to almost twice its natural length. In Fig. 6 the maximum tension is <20 pN, so that the implied assumption of a constant strand length for the analysis is justified. At high flow rates tension could produce significant stretching, but this effect might not significantly affect elution times, because both the driven and resisting strand portions become extended, and peak tension develops only toward the end of elution and near the filter.

All experimental results on which the preceding analysis is based are obtained with the same filter, and the question arises how they might change if other filters were used. Kohn (1991) states that he did not observe any dependence of elution time on the diameter of the filter pores, but he gives no details about the filters used. In the present model the only filter specification needed is not the pore diameter, but the product of pore diameter and pore density that determines the average separation s between pores crossed by a strand on the filter. To assess the consequences of using different filters, a group of eight filters is selected from the manufacturer's catalog; their pore diameter and pore density are listed in Table 3, where no. 5 is the presently used filter. Pore density tends to decrease with increasing pore diameter, but not in a consistent manner; there are three pairs of filters that have the same pore density but different pore diameter. The model elution times T_M are then calculated for these filters and all combinations of three exposures (0, 9, and 54 Gy) and two fragment lengths (0.1 cm for all exposures and a maximum for which the elution time is near 18 h for the particular exposure).

Model elution times T_M are computed based on the resistance parameter R for the selected conditions and obtained for these conditions with filter no. 5. The ratio T_M/T_{M5} (T_{M5} is the value from filter no. 5) is shown in Fig. 7 for 0 and 54 Gy as a function of the filter parameter $p * N$, the number of pores/cm, and for a fragment length of 0.1 cm. The curve for 9 Gy lies between the two curves and is not shown. Vertical lines identify the eight filters, and the two horizontal lines indicate a deviation of ±5%. The common reference point $T_M/T_{M5} = 1$ also is marked. This figure demonstrates that any filter for which $p * N$ is between ~1700 and 3400 could be satisfactorily substituted for filter 5; this includes filters 1, 4, and 6. These limits are more restrictive than those for the longer fragments tried. Note that filter 1, which has the smallest pores, is in the satisfactory group, while the intermediate filters 2 and 3 are not.

TABLE 3 Properties of some polycarbonate filters

Filter no.	p (E-5) (cm)	N (E6) (pores/cm^2)	$p * N$ (pores/cm)
1	1	300	3000
2	2	300	6000
3	4	100	4000
4	6	30	1800
5 *	8	30	2400
6	10	20	2000
7	20	2	400
8	30	2	600

* Filter used in the present experiments.

CONCLUSIONS

The model is based on the idea that only the strand ends are captured by the nearest filter pores and that no intermediate loops are formed. It is also assumed that the acting forces move the entire strand in reptation-like fashion through a channel formed by the immediately surrounding strands.

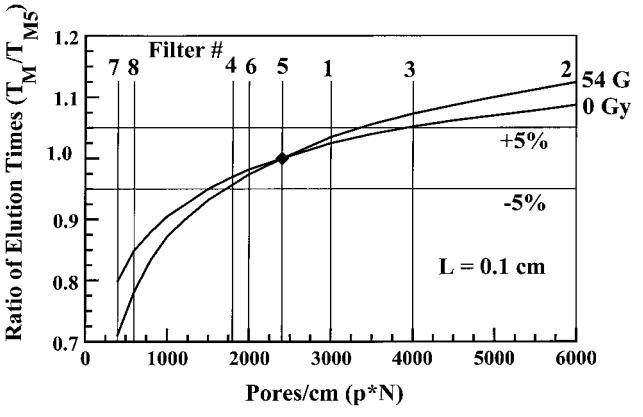

FIGURE 7 Ratio of the elution time for a filter to the elution time for the presently used filter (no. 5) based on the same resistance parameter as that determined for filter no. 5 (Nucleopore 0.8 μm polycarbonate).

Strand motion is treated as quasi-steady, so that the equation of motion is reduced to a balance of driving and resisting forces. The results indicate that both viscosity and strand entanglement on the filter contribute to the resistance to the motion. Resistance from the strand portion on the filter is characterized by an adjustable parameter determined by matching experimental and computed elution times. The model indicates that, for a given exposure, the resistance of fragments increases with fragment length, while the resistance of fragments of a given length increases with exposure. This implies that more and shorter fragments are more easily entangled, possibly contrary to intuition.

A consequence of using a force balance instead of the complete equation of motion is that the computed initial strand velocity cannot be exactly zero, but the approximation is extremely good. To overcome the problems associated with the uncertainty of the flow velocity in the irregular passage behind the filter it is assumed that this flow is constant, but acts only on a portion of the strand. The effect of this assumption on the resistance is quite small (Fig. 4), but it is noticeable for the strand velocity (Fig. 5) and is even more significant for the strand tension (Fig. 6). A different design for the filter support plate is suggested to avoid these difficulties. Experiments with different flow rates are suggested to determine the viscosity and entanglement components of the motion resistance from the strand portion on the filter. Elastic stretching of DNA strands under the influence of the acting forces is shown to be insignificant, at least for the flow rate used in the present experiments.

The mathematical model of the filter elution assay for DNA strand breakage developed here appears to reproduce the main features of the elution phenomenon: an increasing elution time as a function of DNA fragment length, a fragment elution velocity that is a small fraction of the elution velocity during a major portion of the elution time, and a dispersion in elution times for DNA strands of a defined length. The model makes specific numerical predictions for the tension within the strand, resistance parameter values, and strand velocity, but at present there are no data against which to test these predictions. The model also predicts that experimental elution times should vary by not more than $\pm 5\%$ for any filter for which the product of pore diameter and pore density remains within certain limits. Experimental verification of these predictions would lend support for the model. A complete proof would require more elaborate tests; until those become possible, however, we conclude that the concept of reptation, together with classical methods of hydrodynamics, leads to a model for the filter elution of DNA macromolecules that is self-consistent and does not contradict experiment in any obvious manner.

The experimental portion of this study was partially supported by the American Cancer Society, Illinois Division, Inc.(Grants 92-28 and 93-39 to E.R.B.).

REFERENCES

Ahnstrom, G., and K. Erixon. 1973. Radiation induced strand breakage in DNA from mammalian cells. Strand separation in alkaline solution. *Int. J. Radiat. Biol. Relat. Stud. Phys. Chem. Med.* 23:285–289.

Austin, R. H., J. P. Brody, E. C. Cox, T. Duke, and W. Volkmuth. 1997. Stretch genes. *Physics Today.* 5:32–38.

Balbi, C., M. Pala, S. Parodi, G. Figari, B. Cavazza, V. Trefiletti, and E. Patrone. 1986. A simple model for DNA elution from filters. *J. Theor. Biol.* 118:183–198.

Boulton, S., S. Kyle, and B. W. Durkacz. 2000. Mechanisms of enhancement of cytotoxicity in etoposide and ionising radiation-treated cells by the protein kinase inhibitor wortmannin. *Eur. J. Cancer.* 36:535–541.

Bradley, M., and K. W. Kohn. 1979. X-ray-induced DNA double-strand break production and repair in mammalian cells as measured by neutral filter elution. *Nucleic Acids Res.* 7:793–804.

Burki, H., S. Bunker, M. Ritter, and J. E. Cleaver. 1975. DNA damage from incorporated radioisotopes: influence of the 3H location in the cell. *Radiat. Res.* 62:299–312.

Cedervall, B., and P. Källman. 1995. Randomly distributed DNA double-strand breaks as measured by pulsed field gel electrophoresis: a series of explanatory calculations. *Radiat. Environ. Biophys.* 33:9–21.

Clift, R., J. R. Grace, and M. W. Weber. 1978. Bubbles, Drops and Particles. Academic Press, New York.

Contopoulou, C. R., V. E. Cook, and R. K. Mortimer. 1987. Analysis of DNA double strand breakage and repair using orthogonal field alternation gel electrophoresis. *Yeast.* 3:71–76.

Crowe, C., Y. Sommerfeld, and Y. Tsuji. 1997. Multiphase Flows with Droplets and Particles. CRC Press, Boca Raton, FL.

Dasika, G. K., S. C. Lin, S. Zhao, P. Sung, A. Tompkinson, and E. Y. Lee. 1999. DNA damage-induced cell-cycle checkpoints and DNA strand break repair in development and tumorigenesis. *Oncogene.* 18: 7883–7899.

de Gennes, P. G. 1971. Reptation of a polymer chain in the presence of fixed obstacles. *J. Chem. Phys.* 55:572–579.

Duke, T. A. J., R. H. Austin, E. C. Cox, and S. S. Chan. 1996. Pulsed-field electrophoresis in microlithographic arrays. *Electrophoresis.* 17: 1075–1079.

Dwight, H. B. 1953. Tables of Integrals and Other Mathematical Data. Macmillan Co., New York.

Fan, L-S., and C. Zhu. 1998. Principles of Gas-Solid Flows. Cambridge University Press, Cambridge, U.K.

Fuchs, N. A. 1989. The Mechanics of Aerosols. Dover Publications, Mineola, New York. (Originally published 1964 by Macmillan Co., New York, New York.)

Gray, H. B., V. A. Bloomfield, and J. E. Hearst 1967. Sedimentation coefficients of linear and cyclic wormlike coils with excluded volume effects. *J. Chem. Phys*. 46:1493–1498.

Kantor, R. M., X. H. Guo, E. J. Huff, and D. C. Schwartz. 1999. Dynamics of DNA molecules in gels studied by fluorescence microscopy. *Biochem. Biophys. Res. Commun*. 258:102–108.

Kaur, B. S., and E. R. Blazek. 1997. Subdenaturing (pH 11.1) filter elution: more sensitive quantification of DNA double-strand breaks. *Radiat. Res.* 147:569–578.

Kiltie, A. E., C. J. Orton, A. G. Ryan, S. A. Roberts, B. Marples, S. E. Davidson, R. Hunter, G. P. Margison, C. M. L. West, and J. Hendry. 1997. A correlation between residual DNA double-strand breaks and clonogenic measurements of radiosensitivity in fibroblasts from preradiotherapy cervix cancer patients. *Int. J. Radiat. Oncol. Biol. Phys.* 19:1137–1141.

Kohn, K. W. 1979. DNA as a target in cancer chemotherapy: measurement of macromolecular DNA damage produced in mammalian cells by anticancer agents and carcinogens. *Meth. Cancer Res.* 16:291–345.

Kohn, K. W. 1991. Principles and practice of DNA filter elution. *Pharmacol. Ther.* 49:55–77.

Kohn, K. W. 1996. DNA filter elution: a window on DNA damage in mammalian cells. *BioEssays.* 18:505–513.

Kohn, K. W., L. Erickson, R. Ewig, and C. Friedmann. 1976. Fractionation of DNA from mammalian cells by alkaline elution. *Biochemistry.* 15: 4629–4637.

Kohn, K. W., and R. A. Grimeg-Ewig. 1973. Alkaline elution analysis, a new approach to the study of DNA single-strand interruptions in cells. *Cancer Res.* 33:1849–1853.

Lett, J., I. Caldwell, C. Dean, and P. Alexander. 1967. Rejoining of x-ray induced breaks in the DNA of leukemia cells. *Nature.* 214:790–792.

Löbrich, M., S. Ikpeme, and J. Kiefer. 1994. Measurement of DNA double-strand breaks in mammalian cells by pulsed-field gel electrophoresis: a new approach using rarely cutting restriction enzymes. *Radiat. Res*. 138:186–192.

Mayer, P. J., C. S. Lange, M. O. Bradley, and W. W. Nichols. 1991. Investigation of the neutral filter elution technique. I. Effects of pore density and pore diameter on elution rate at pH 9.6. *Radiat. Res.* 125:197–205.

McDonell, M., M. Simon, and F. Studier. 1977. Analysis of restriction fragments of T7 DNA and determination of molecular weights by electrophoresis in neutral and alkaline gels. *J. Mol. Biol.* 110:119–146.

Nevaldine, B., J. A. Longo, and P. J. Hahn. 1997. The scid defect results in much slower repair of DNA double-strand breaks but not high levels of residual breaks. *Radiat. Res.* 147:535–540.

Nicolini, C., A. Belmont, S. Zietz, A. Maura, A. Pino, L. Robbiano, and G. Brambilla. 1983. Physico-chemical model for DNA alkaline elution: new experimental evidence and differential role of DNA length, chain flexibility and superpacking. *J. Theor. Biol.* 100:341–357.

Painter, R. B. 1980. The role of DNA damage and repair in cell killing induced by ionizing radiation. *In* Radiation Biology in Cancer Research. Raymond E. Meyn and Rodney H. Withers, editors. Raven Press, NY. 59–68.

Perkins, T. T., D. E. Smith, and S. Chu. 1994. Direct observation of tube-like motion of a single polymer chain. *Science.* 264:819–822.

Rudinger, G. 1980. Fundamentals of gas-particle flow. *In* Handbook of Powder Technology, Vol. 2. Elsevier Scientific Publishing Co., Amsterdam, The Netherlands.

Schwartz, D. C., and C. R. Cantor. 1984. Separation of yeast chromosome-sized DNAs by pulsed field gradient gel electrophoresis. *Cell.* 37:67–75.

Simon, J. A., P. Szankasi, D. K. Nguyen, C. Ludlow, H. M. Dunstan, C. J. Roberts, C. Jensen, L. H. Hartwell, and S. H. Friend. 2000. Differential toxicities of anticancer agents among DNA repair and checkpoint mutants of *Saccharomyces cerevisiae. Cancer Res.* 60:328–333.

West, C. M. L. 1995. Invited review: Intrinsic radiosensitivity as predictor of patient response to radiotherapy. *Br. J. Radiol.* 68:827–837.

Zimm, B. 1974. Anomalies in sedimentation. IV. Decrease in sedimentation coefficients of chains at high fields. *Biophys. Chem.* 1:279–291.

Zimm, B., and V. Schumaker. 1976. Anomalies in sedimentation. V. Chains at high fields, practical consequences. *Biophys. Chem.* 5:265–270.